Dynamics of active magmatic and hydrothermal systems at Taal Volcano, Philippines, from continuous GPS measurements

Beth A. Bartel,[1,2] Michael W. Hamburger,[1] Chuck M. Meertens,[3] Anthony R. Lowry,[4] and Ernesto Corpuz[5]

Received 9 September 2002; revised 27 February 2003; accepted 28 April 2003; published 16 October 2003.

[1] A dense network of continuous single- and dual-frequency GPS receivers at Taal Volcano, Philippines, reveals four major stages of volcanogenic deformation: deflation, from installation in June 1998 to December 1998; inflation, from January to March 1999; deflation, from April 1999 to February 2000; and inflation, from February to November 2000. The largest displacements occurred during the February–November 2000 period of inflation, which was characterized by ~120 mm of uplift of the center of Volcano Island relative to the northern caldera rim at average rates up to 216 mm/yr. Deformation sources were modeled using a constrained least squares inversion algorithm. The source of 1999 deflation and inflation in 2000 were modeled as contractional and dilatational Mogi point sources centered at 4.2 and 5.2 km depth, respectively, beneath Volcano Island. The locations of the inflationary and deflationary sources are indistinguishable within the 95% confidence estimates. Modeling using a running 4-month time window from June 1999 to March 2001 reveals little evidence for source migration. We suggest that the two periods of inflation observed at Taal result from episodic intrusions of magma into a shallow reservoir centered beneath Volcano Island. Subsequent deflation may result from exsolution of magmatic fluids and/or gases into an overlying, unconfined hydrothermal system. *INDEX TERMS:* 1208 Geodesy and Gravity: Crustal movements—intraplate (8110); 1294 Geodesy and Gravity: Instruments and techniques; 8145 Tectonophysics: Physics of magma and magma bodies; 8434 Volcanology: Magma migration; 9320 Information Related to Geographic Region: Asia; *KEYWORDS:* volcano, geodesy, deformation, GPS, Taal

Citation: Bartel, B. A., M. W. Hamburger, C. M. Meertens, A. R. Lowry, and E. Corpuz, Dynamics of active magmatic and hydrothermal systems at Taal Volcano, Philippines, from continuous GPS measurements, *J. Geophys. Res.*, *108*(B10), 2475, doi:10.1029/2002JB002194, 2003.

1. Introduction

[2] Understanding magmatic systems in detail requires ample spatial and temporal density of measurements. Within the past 30 years, the advent of continuous instruments such as tiltmeters, strain meters, and, more recently, the Global Positioning System (GPS) has enabled both high temporal density and remote measurements with minimal risk to personnel. Spatial densification of GPS networks, as with the other continuous methods, has been limited by instrument costs. To overcome this obstacle, a low-cost, single-frequency (L1) GPS system was developed by UNAVCO [*Meertens et al.*, 1998]. This system was subsequently implemented at a small number of volcanoes worldwide, including Long Valley, California [*Meertens et al.*, 1999]; Popocatéptl, Mexico [*Cabral-Cano et al.*, 1999]; Kilauea/Mauna Loa, Hawaii [*Cervelli et al.*, 2002]; Erebus, Antarctica; Sierra Negra, Galapagos; and Taal Volcano, Philippines [*Bartel et al.*, 1999]. The continuous GPS network at Taal now consists of three dual-frequency sites for high-precision measurements of key points and eleven single-frequency sites for network densification, making the combined GPS networks at Taal one of the densest volcano-monitoring networks in the world. In this paper, we report on the first 3 years of continuous GPS observations at Taal Volcano.

[3] The geometry of the magmatic system, the influence of regional tectonics, and the currently active magmatic processes at Taal remain poorly understood despite several previous seismic and deformation studies. A history of volcanogenic deformation at Taal, most recently in volcanic crises in 1992 and 1994, suggests that detailed deformation studies are likely to yield rich data sets that will help address these questions. Frequent unrest, a long history of deformation, a variety of eruptive styles, and accessibility of sites close to the center of activity make Taal an ideal laboratory for the detailed study of deformation related to volcanic systems. In this paper, we attempt to improve our understanding of the geometry of

[1]Department of Geological Sciences, Indiana University, Bloomington, Indiana, USA.
[2]Now at UNAVCO, Inc., Boulder, Colorado, USA.
[3]UNAVCO, Inc., Boulder, Colorado, USA.
[4]Department of Physics, University of Colorado, Boulder, Colorado, USA.
[5]Philippine Institute of Volcanology and Seismology, Department of Science and Technology, Quezon City, Philippines.

0148-0227/03/2002JB002194$09.00

the magmatic system and of the processes of magma recharge at Taal Volcano through analysis of 3.5 years of continuous dual- and single-frequency GPS data.

2. Volcano-Tectonic Setting

[4] Taal Volcano is a complex stratovolcano located only 60 km south of metropolitan Manila. Earlier Cenozoic volcanism at Taal was a product of eastward subduction of the South China Sea crust at the Manila Trench west of Luzon (Figure 1). More recent volcanism relates to the so-called ''Macolod Corridor,'' a zone of presumed extension or shear associated with the southern terminus of the Manila Trench subduction zone, and cutting northwest across southern Luzon [*Defant et al.*, 1988]. The Taal volcanic system consists of the ~5 km diameter Volcano Island within the large (~15 × 25 km), caldera-filling Lake Taal. All historical activity has been associated with Volcano Island, from volcanic centers aligned along two lineaments crossing the island. These lineaments intersect at the island's lake-filled Main Crater (Figure 1) [*Alcaraz*, 1966; *Alcaraz and Datuin*, 1974]. Caldera-scale activity as recently as 5.3 ka was responsible for widespread ignimbrites which now underlie parts of Metro Manila [*Wolfe and Self*, 1983; *Listanco*, 1994]. Future potential for caldera-scale activity is unknown.

[5] At least 33 eruptions have been recorded at Taal since its first documented activity in 1572 [e.g., *Punongbayan and Tilling*, 1989]. Eruptions have been predominantly phreatic and phreatomagmatic; products are commonly basalt and basaltic andesite, though erupted materials have ranged to dacite [*Miklius et al.*, 1991]. The most recent eruption sequence, from 1965 to 1977, began in 1965 with phreatomagmatic activity accompanied by a violent base surge. The activity opened a new eruption center on the southwest flank of Volcano Island [*Moore et al.*, 1966]. For an overview of Taal's eruption history, see *Torres et al.* [1995].

[6] Recent activity, such as geysering, seismicity, deformation, and changes in water chemistry and temperature indicate the presence of shallow magma beneath Taal. Most notably, two episodes of unrest occurred in 1992 and 1994 and consisted of intense seismicity, sudden ground deformation, and changes in lake temperature and chemistry [*Gabinete*, 1999]. In 1992, up to 21 cm of uplift in <1 day was measured along the shores of Volcano Island through EDM, precise leveling, and water well measurements [*Gabinete*, 1999]. Locations of seismic events associated with the 1994 crisis cluster along a northwest-southeast oriented zone across Volcano Island, with 92% of events located within 3 km of the surface [*Tieman*, 1999]. Both crises are believed to relate to dike intrusions; neither crisis culminated in eruption. EDM and leveling surveys made by PHIVOLCS since these crises indicate a general long-term trend of deflation, though with shorter-term variability. Similarly, campaign GPS surveys in 1996 and 1998 indicate cumulative deflation, yet surveys in 1998 and 1999 indicate little to no motion [*Bartel*, 2002]. Without more frequent measurements, it is impossible to ascertain the duration or magnitude of these short-term deformation trends, or even determine whether the long-term trend at Taal is toward deflation or inflation.

[7] Past studies of subsurface structure of the Taal region are few. A zone of partial melt at 18 km depth beneath the Taal region was inferred from results of a shear wave splitting survey [*Besana et al.*, 1995]; they noted that the limited data may also be fit by a deeper zone of partial melt and a shallower Moho discontinuity. *Nishigami et al.* [1994] inferred a shallower region of melt with a fan-shooting seismic refraction survey, interpreting the upper bounds of a region of low velocity and high attenuation at ~1 km depth beneath Taal's Main Crater and strong reflectors at 7–10 km beneath the caldera. *Lowry et al.* [2001] suggested that this observed reduction in velocity at shallow depths may result not from partial melt but from hydrothermal alteration of the near-surface crust in this vicinity. Thus the depth to shallow magma bodies beneath Taal remains ambiguous.

3. GPS Networks

[8] In May 1998, a continuous dual-frequency network (Figure 1) was installed on Volcano Island consisting of three sites: KAYT, TVST, and PINT. The instruments were installed approximately equidistant from the volcano's center, on opposing flanks of Volcano Island, to maximize the aperture and azimuthal coverage of the network. One year later, in June 1999, eight L1 sites (TV01, TV02, TV03, TV04, TV05, TV06, and TV12) were installed on Volcano Island, with three additional sites (TV08, TV10, and TV11) installed around the caldera rim. An example of one of the L1 sites is shown in Figure 2. While the dual-frequency GPS network offers high-precision geodetic data at a few key points, and long baseline ties to regional networks, the L1 network offers short baseline network densification, and measurements in key points where instrument loss due to volcanic activity is possible. Because of the volcano's gentle terrain and accessibility, we have been able to establish measurement sites within 0.5 km of the volcano's center and at a wide variety of azimuths from the volcano's Main Crater. Details of the two networks' instrumentation and operation are provided by *Bartel* [2002]. Since installation, the network has been modified due, in part, to vandalism. Twelve sites operate at the time of this writing.

4. Data Processing

[9] The continuous Taal data is processed for daily coordinate solutions, formal errors, and data covariances using Bernese version 4.2 software [*Hugentobler et al.*, 2001]. The three dual-frequency sites are processed together with two continuous sites in Manila, MMA8 (also named MANL) and PIMO. These Manila sites provide reference to a region not affected by volcano deformation. Relative positions are estimated on baselines referenced to KAYT, which has the most continuous measurement time series. Data are first processed using the immediately available IGS rapid orbit prediction combinations for precise orbit and pole information and subsequently reprocessed using more precise IGS final orbit and pole combinations [*Beutler et al.*, 1995] as they become available. Data are processed in a standard sequence including cycle-slip screening and outlier removal, troposphere estimation, ambiguity resolution, and a network solution for daily site coordinates [*Lowry et al.*, 2001]. All L1 data (including that of the dual-frequency

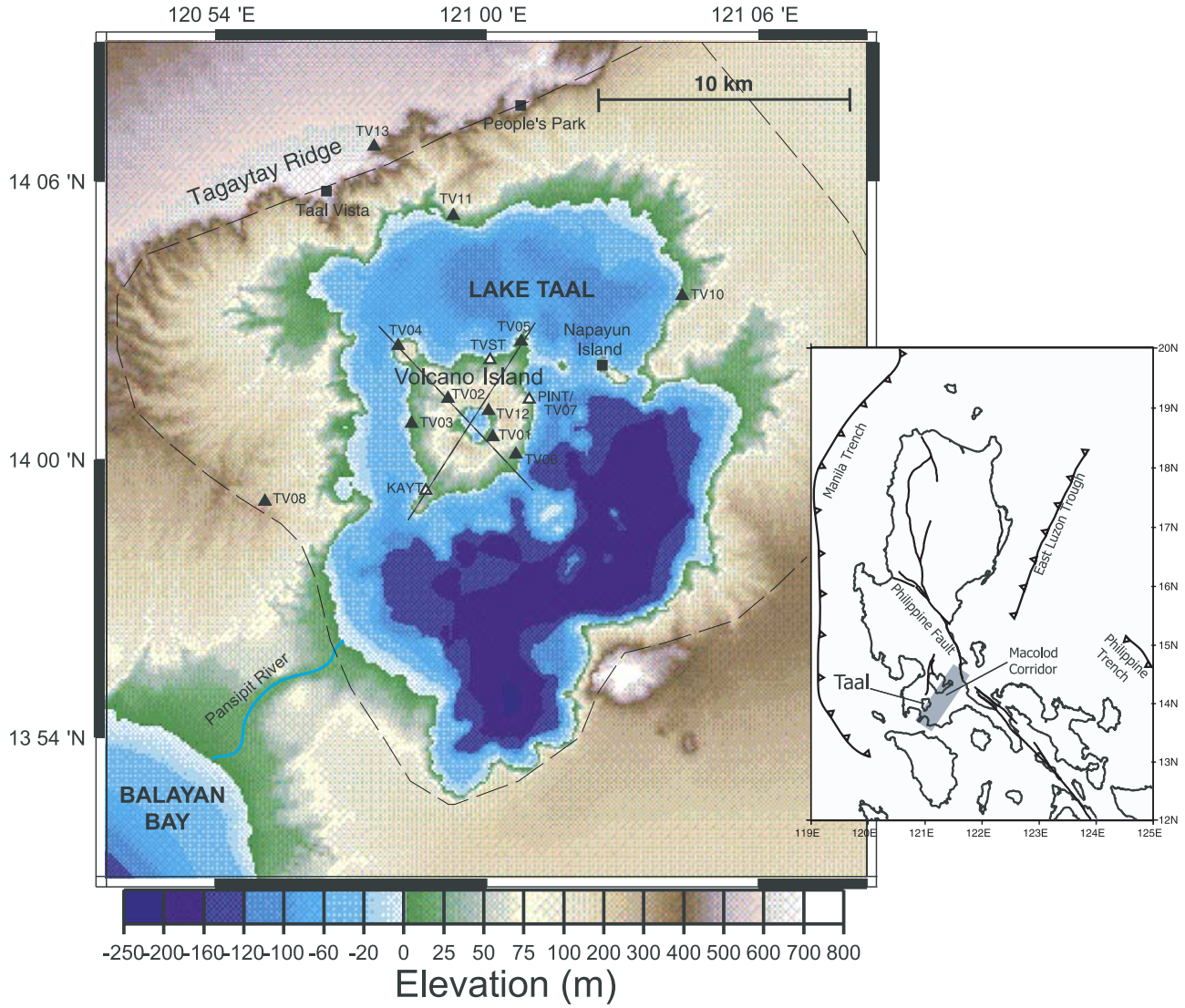

Figure 1. Digital elevation map of Taal Volcano and vicinity, with continuous GPS networks. Dual-frequency GPS sites are shown as open triangles; single-frequency GPS sites are shown as solid triangles. Black squares indicate repeater sites. Dashed lines crossing Volcano Island indicate alignment of eruption centers [after *Alcaraz*, 1966]; approximate boundaries of Taal caldera are shown by dashed lines surrounding Lake Taal [after *Torres et al.*, 1995]. Inset shows the regional tectonic setting and the location of Taal on the island of Luzon. (Digital elevation model provided by E. Ramos, PHIVOLCS.)

sites) are processed together for daily coordinate solutions and covariances. Because we cannot eliminate ionospheric effects using the L1 data alone, we apply a global ionosphere model (GIM) in our final parameter estimation. The GIM is made available via ftp within ~4 days by the Center for Orbit Determination in Europe (CODE), one of the Analysis Centers of the International GPS Service for Geodynamics (IGS) [*Schaer et al.*, 1996]. Although the resolution of the GIM is too coarse to remove all ionospheric effects at Taal, we apply the model to remove a scale factor affecting the entire network. We process the single-frequency data without estimation of site-specific tropospheric parameters because we find that assimilation of unmodeled ionospheric effects into the estimates of tropospheric delays generally increases scatter in the data [*Bartel*, 2002]. Formal error estimates on site coordinates are scaled to coordinate repeatability calculated from detrended time series. Scale factors are computed for each component at each station.

5. Network Precision

[10] Because the use of single-frequency GPS in geodetic applications is still relatively new, it is worth commenting here on measurement precision. We find that scatter in the vertical component increases approximately linearly with increasing baseline length, from a coordinate repeatability of 5 mm for a 2.8 km baseline to 18 mm for a 13.3 km baseline. East component repeatability ranges from 2 mm to 6 mm for the same range of baseline lengths. North component repeatability is significantly higher than that of the east component, and appears to depend on distance

Figure 2. Single-frequency site set-up. Shown is site TV12, within the Main Crater. Contents of the stainless steel box include CMC GPS receiver housed together with FreeWave radio modem (A), and deep cycle battery (B). (Photographs by M. Hamburger.)

north from the base station KAYT rather than on total baseline length. RMS scatter ranges from 3 mm for a latitude aperture of0.6 km to 15 mm for a 9.8 km aperture. The greater north component scatter in L1 coordinate solutions is probably the result of small-scale ionospheric effects. Taal is at low latitudes (~14°N) where the gradient in ionospheric total electron content is generally greatest along north-south azimuths [e.g., *Kelley*, 1989]. Figure 3 compares results of dual- versus single-frequency processing. Peak-to-peak scatter in the vertical component is roughly comparable in both cases, while scatter in the east and, in particular, north components of the coordinate solutions is greater in the L1-only processing. Note that, despite increased scatter, the ~30 mm deformation signal is still clearly discernable in the L1 data.

6. Deformation Trends at Taal, 1998–2002

[11] Although there has been no eruption within the time period studied here, the continuous data from the Taal Volcano GPS networks reveal highly time variable deformation of the volcanic edifice. Major trends include two episodes of inflation separated by two episodes of deflation, indicated by northeastward and southwestward motion, respectively, of all sites relative to base station KAYT (Figures 4 and 5). The four major deformation trends can be summarized as follows: deflation from installation in June 1998 to December 1998 (minimum 7 months); inflation from January to March 1999, accelerating in February (~2 months total); deflation from April 1999 to January 2000 (~10 months); and inflation from February to November 2000 (~9 months). Deflation in both cases began gradually and is characterized by an irregular rate. Inflation began and ended abruptly and was characterized by near-constant velocity that exceeded that of the deflationary trends. The lack of annual cyclicity argues against a seasonal mechanism.

[12] Figure 6 compares the timing of deformation to seismic and hydrothermal activity. The most notable activity has consisted of: (1) several spectacular geysering episodes in August 1998 and February 1999 from a hydrothermal vent within the Main Crater, consisting of mud fountaining of up to 6 m, not accompanied by notable changes in seismicity; (2) near-daily geysering from the same vent for 1 year (February 1999 to February 2000); and (3) two periods of increased seismicity and intensified geysering. The latter included elevated levels of seismicity in July–August 1999 accompanied by a temperature increase of 4–6°C in hydrothermal vent waters (Taal Volcano Advisory, PHIVOLCS, 30 September 1999), and a seismic swarm of 484 recorded events from 24 September to 4 October 1999. The relationship between deformation trends and these other observables is ambiguous. The 1999 seismicity occurred during the yearlong deflationary trend but was not associated with any notable perturbation of that trend (see east components of the PINT and TVST time series, Figure 4). A more substantial correlation exists between deformation and major changes in hydrothermal behavior. *Lowry et al.* [2001] noted that mud fountaining in February 1999 coincided with the peak of the first recorded inflationary trend (Figures 4 and 6). Approximately 2 weeks later, inflation ceased abruptly and gave way to deflation; deflation and near-daily geysering continued for ~1 year, with geysering ceasing 2 weeks after initiation of the second inflationary trend (approximately 1 February and 19 February 2000, respectively; see Figure 6).

[13] Notably, the first period of inflation (and accompanying initiation of geysering), in February 1999, was accompanied by no unusual seismicity. A slight increase in seismicity above base level was noted beginning in

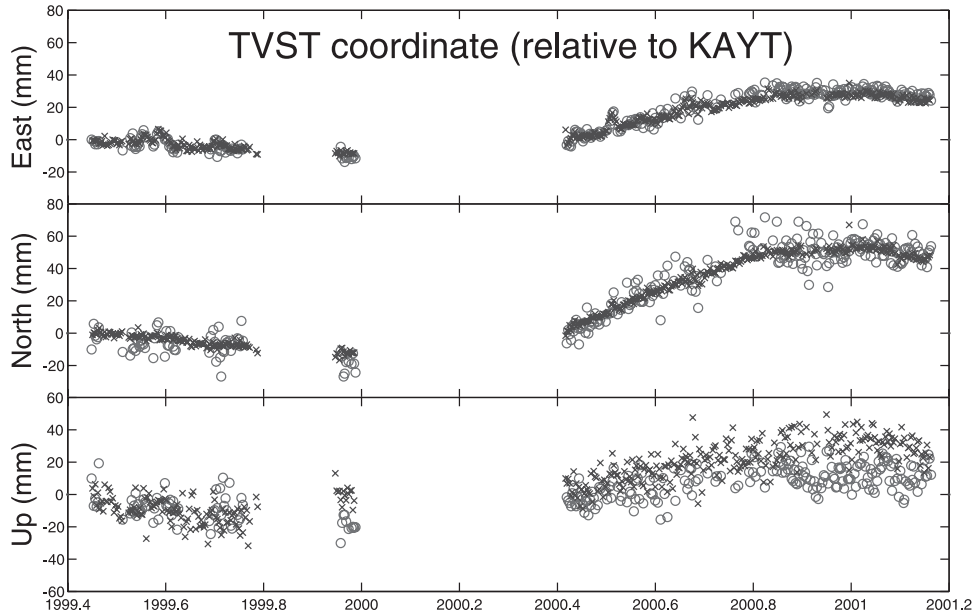

Figure 3. Comparison of dual- versus single-frequency data processing. Daily coordinate solutions obtained for dual-frequency site TVST relative to dual-frequency site KAYT, using both the L1 and L2 frequencies (crosses) versus using only the L1 frequency (circles). Differences in processing are described in the text.

August 2000, ~6 months after initiation of February–November 2000 inflation (Figures 4 and 6). Similarly, uplift at Long Valley caldera preceded an increase in seismic moment in both 1989 [*Langbein et al.*, 1993] and in 1997–1998 [*Newman et al.*, 2001]. *Barberi et al.* [1984] noted that uplift at Campi Flegrei beginning in June 1982 preceded an increase in seismic energy release and earthquake rate by 9 months. This behavior suggests that significant changes within the magmatic system may be recognizable in the deformation data well before they are evidenced by changes in seismic activity.

7. Site Velocities and Source Modeling

[14] For the remainder of the analysis, we focus on the single-frequency data available from network installation in June 1999 through 1 March 2001, when network density is the highest (Figure 5). This 21-month (1.75 year) period contains the 1999 deflationary trend and the 2000 inflationary trend (Figure 6a). Three-dimensional site velocities and corresponding 95% confidence estimates were calculated for each trend using a standard weighted least squares method with the full data covariance; velocities were then used as input to invert for source parameters based on a simple Mogi point source model. All operations were executed using DisModel, a program developed in Matlab by P. Cervelli and J. Murray of the Crustal Deformation group of Stanford University [*Cervelli et al.*, 2002].

[15] All site velocities were calculated relative to dual-frequency site KAYT, located just 3 km from the volcano's Main Crater. DisModel correctly models these relative velocities, but horizontal velocities depicted in Figures 7 and 8 are shown in a local "volcanic" reference frame in which an average network velocity was subtracted from each site velocity for each time period. Results are given in Table 1 and shown in Figures 7 and 8. The average network velocity is represented (in opposite polarity) as the velocity of base station KAYT.

[16] During both the 1999 deflationary trend and the 2000 inflationary trend, motions were radial from the center of Volcano Island with the largest horizontal motions at sites on the periphery of Volcano Island and the largest vertical velocities at sites central to Volcano Island. Deflation in 1999 produced over 40 mm/yr of horizontal shortening between sites on opposite shores of Volcano Island (southwestern site KAYT and northeastern sites TVST, TV05, and PINT). Differencing vertical velocities between caldera rim site TV08 and island sites TV05, TV06, and TV12, indicates subsidence of island sites relative to the caldera rim at rates up to ~30 mm/yr. In contrast, inflation in 2000 was characterized by ~140 mm/yr of horizontal lengthening between sites on opposite shores of Volcano Island (southwestern site KAYT and northeastern sites TVST and TV05). Motion estimated for the same stations from the time series in Figure 5 indicates lengthening of up to 80 mm east and 75 mm north across Volcano Island. Vertical motions at the sites along the caldera rim (TV08, TV10, and TV13) are downward relative to KAYT, opposite in sign from the sites on Volcano Island, reflecting upward motion of KAYT relative to the caldera rim. Differencing the vertical velocities of site TV13, on the northern rim of the caldera, and site TV12, the site nearest the center of Volcano Island, yields an uplift rate of ~220 mm/yr of Volcano Island relative to the caldera rim. Motion estimated for the same stations from the time series in Figure 5 reveals ~120 mm of total uplift in the 9-month period. The uplift rate is comparable to the ~200 mm/yr estimated from leveling surveys for the 1979–1980 crisis period at Long Valley caldera [*Castle et al.*, 1984]. It is also similar to the average long-term uplift rate of ~150 mm/yr measured from 1971 to

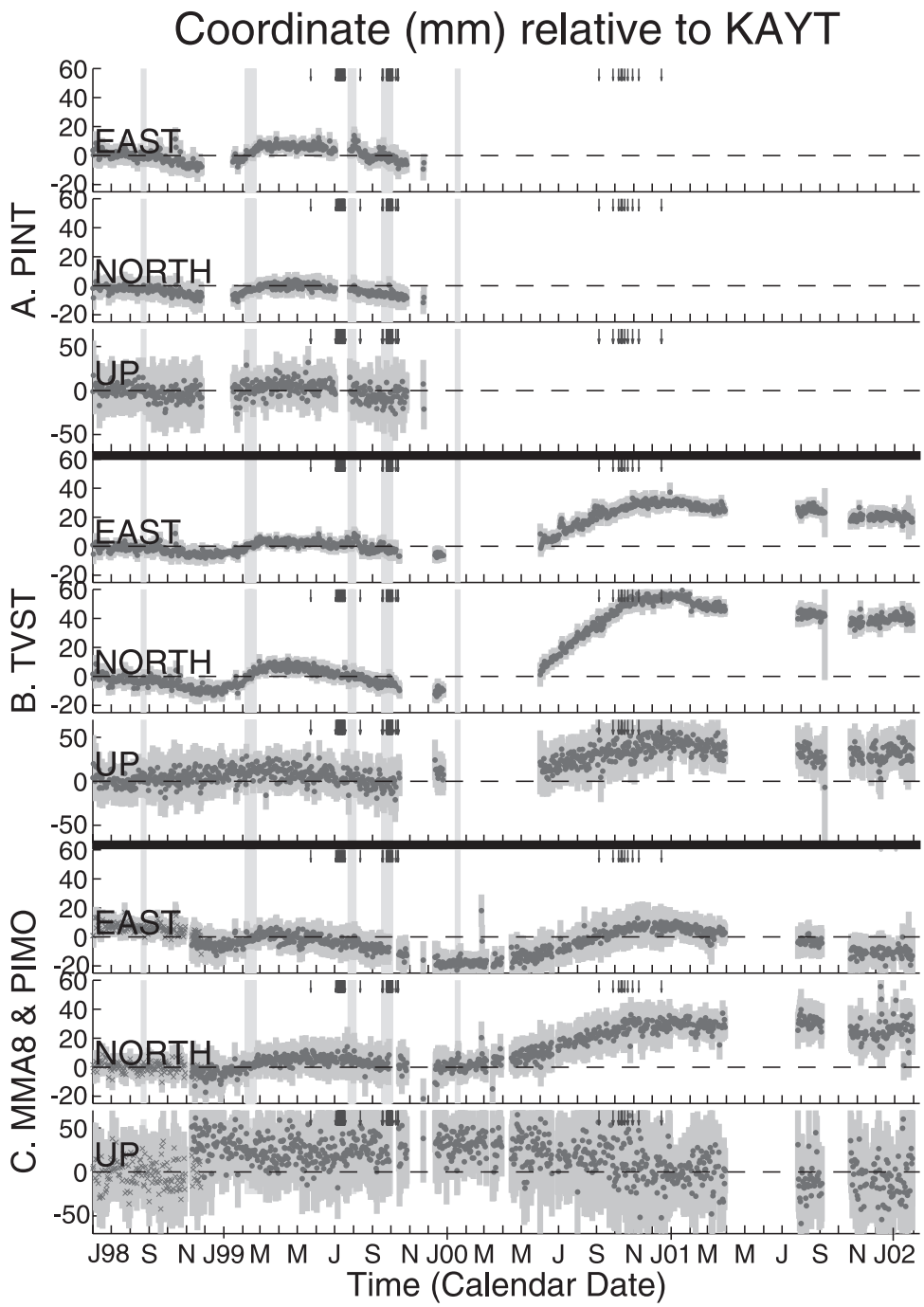

Figure 4. Time series of dual-frequency site coordinate change relative to KAYT, June 1998 to February 2002. Dark dots are daily solutions; medium gray bars are 95% formal error scaled to repeatability. Light gray bands indicate periods of anomalous hydrothermal activity, arrows denote >5 local high-frequency earthquakes per day (data available for January 1999 to February 2001 only). Note that the scale factor for the vertical coordinate is twice that for horizontal. (a) PINT; (b) TVST; (c) Manila sites (crosses, MMA8; circles, PIMO).

1983 (prior to the crisis of 1983–1985) and again from 1993 until the 1994 eruption at Rabaul caldera [*Rabaul Volcano Observatory*, 1994].

[17] The original observed site velocities (both horizontal and vertical) were used to invert for Mogi source parameters. The model predicts displacements at the surface resulting from a pressure change within a spherical point source embedded in a semi-infinite, homogenous, elastic half-space [*Mogi*, 1958]. A best fit source to match the observed deformation is obtained through a Levenberg-Marquardt constrained least squares inversion algorithm that minimizes the misfit between model and observed deformation rates. We use a starting model centered beneath Volcano Island's Main Crater (see Table 2). We find that

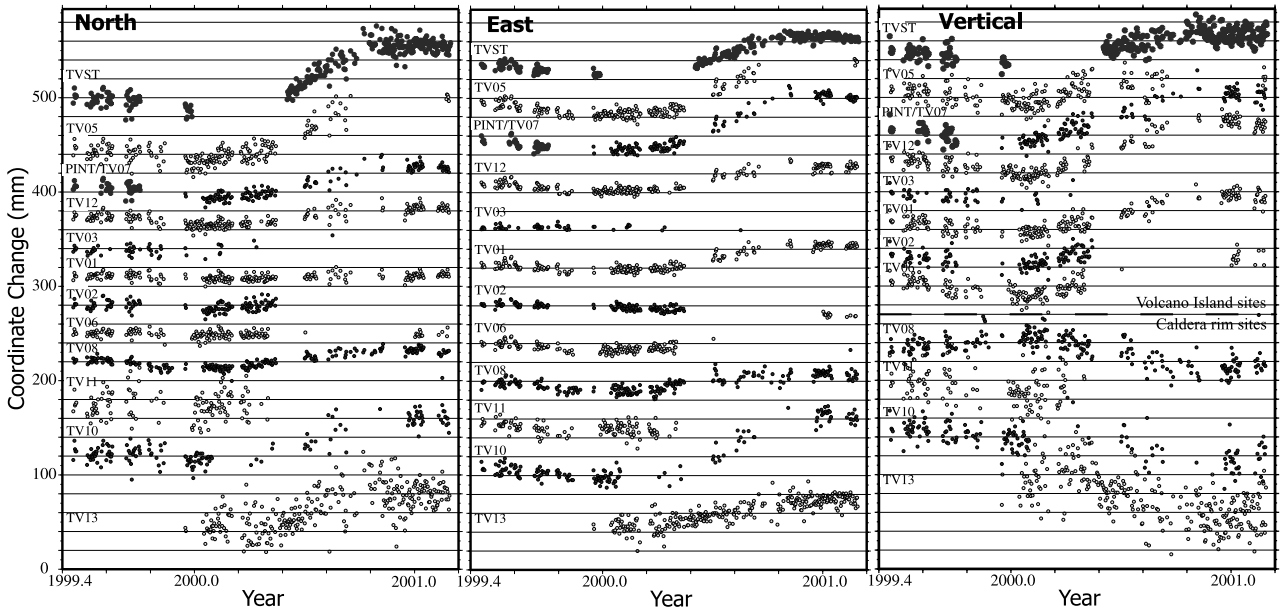

Figure 5. Time series of single-frequency site coordinate change relative to KAYT, June 1998 to February 2001. For clarity, errors are not shown but can be estimated based on repeatability.

varying the initial estimate of Mogi source location laterally beneath Volcano Island has little or no effect on the solution. Initial location estimates > ~10 km from the volcano's center can fall prey to local minima in the solution space that are both volcanically unrealistic and yield a poorer fit to the observed data.

[18] The quality of the model fit to the observed data is expressed as the mean square error (MSE). We estimate the 95% confidence interval for each model parameter by comparing the MSE R^2 for a range of models to the minimum MSE $R^2_{\min}$ via the likelihood ratio method [*Beck and Arnold*, 1977]. If errors are jointly normal, zero mean, and uncorrelated, then the confidence region having probability α of containing the solution corresponds to the volume of the model parameter space for which

$$R^2 \leq R^2_{\min}\left[1 + M F_{\alpha}^{-1}(M, n-M)/(n-M)\right], \qquad (1)$$

in which M is the number of model parameters, n is the number of measurements, and F^{-1} is the inverse of the F cumulative distribution function. Results of this parameter analysis are shown in Figures 9 and 10.

[19] Inversion results indicate that both the 1999 deflationary and 2000 inflationary deformation sources are centered beneath Volcano Island. The source of deflation is centered at 4.2 +3.6/−2.0 km depth, slightly southeast of the Main Crater (Table 2 and Figure 7), while the source of inflation is estimated at a depth of 5.2 +3.9/−2.0 km, slightly northeast of the Main Crater, within 2 km horizontally and 1 km vertically of the deflationary source; the two sources are indistinguishable within the 95% confidence estimates (Table 2 and Figure 8). The depth range is roughly consistent with the depths of deformation sources determined from both uplift and subsidence recorded at Taal since 1994. *Gabinete* [1999] modeled deformation associated with the 1994 crisis as pressurization of a point source at 5 km depth beneath the volcano's Main Crater, attributing the crisis to intrusion of magma from a deeper reservoir to shallower depths. The post-1994 deflation measured in campaign GPS data from 1996 and 1998 was described by *Thibault* [1999] as depressurization of a point source at 3 km depth beneath the southeast flank of Volcano Island, centered at the base of the 1994 seismic activity. *Lowry et al.* [2001] modeled the early continuous dual-frequency GPS data (June 1998 to October 1999) using a simple Mogi point source. Inversions revealed variable deformation behavior switching between deflationary and inflationary sources with most high-confidence source locations at ~2–5 km depth and centered beneath Volcano Island.

7.1. Multiple Sources

[20] In an attempt to resolve more complex magma sources, we examined two alternative modeling approaches. First, we attempted to model the deformation associated with the 2000 inflation using a dilatational dislocation along a plane (dike source). Results suggest that the inflationary episode may be better modeled as an elongate source oriented NW-SE, consistent with the orientation of seismicity and fissures associated with the 1994 crisis and with one of the two proposed lineaments crosscutting Volcano Island. Second, the 2000 deflationary and inflationary trends were modeled again using only the outer (caldera rim) sites versus using only the inner (Volcano Island) sites. The motivation for this test was a search for possible deeper sources of deformation. A deeper source should dominate deformation recorded at the outer sites, while a shallower source should primarily affect deformation at the inner sites. For the 2000 inflationary trend, results obtained for both outer and inner data sets are reasonable when compared to the best fit model obtained using all stations and are indistinguishable within the 95%

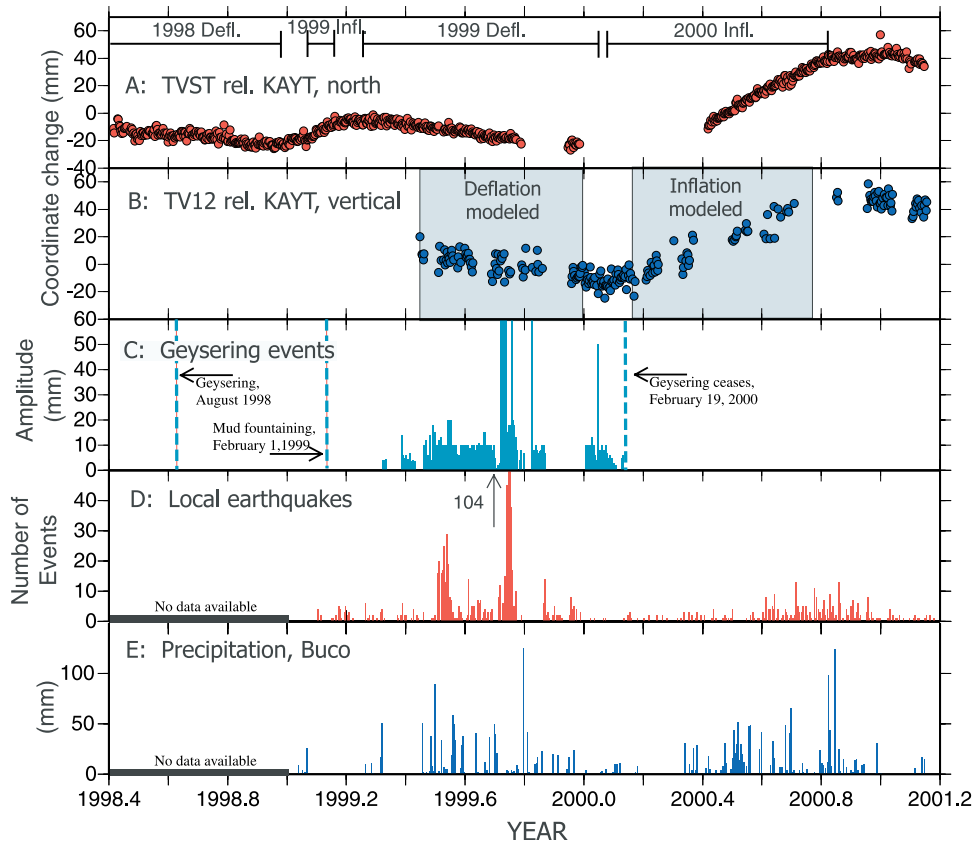

Figure 6. Comparison of observed volcanic and meteorological parameters, June 1998 to February 2001. (a) Position of TVST relative to KAYT, north coordinate component, as shown in Figure 4. Time periods of deflation and inflation are referenced in text. (b) Position of TV12 relative to KAYT, vertical coordinate component, as shown in Figure 5. Gray boxes indicate time periods modeled. (c) Geysering events from the hydrothermal vent within the Main Crater, represented by the amplitude of shaking recorded on a seismic instrument within the Main Crater (maximum amplitude 60 mm), noted beginning April 1999. Initiation and cessation of geysering are indicated by dashed vertical lines. (d) Number of local earthquakes per day, based on three-station seismic network operated by PHIVOLCS, beginning in January 1999. (e) Daily precipitation as recorded at Buco, on the northern shore of Lake Taal, beginning in January 1999. All ancillary data were provided by PHIVOLCS.

confidence estimates (6.3 km, 95% confidence range of ~4–11 km depth and 4.7 km, 95% confidence range of ~3–10 km depth, respectively). Thus we find no evidence for further complexities in the shallow magmatic reservoir system, such as an additional, deeper reservoir at ~8–10 km depth as suggested by seismic studies and deformation data from 1992 to 1994.

7.2. Time-Variable Deformation

[21] We also explored possible time variability of the source through modeling of velocities determined for 4-month time windows staggered at 1-month intervals throughout the time period from June 1999 through February 2001 (Figure 11 and Table 3). Again, we use a simple Mogi model to describe deformation. All deformation sources for the running time windows fall close to or east of the center of the volcano, centered beneath Volcano Island during time periods when the signal-to-noise ratio is high. Three outliers, located on the northwestern and northeastern flanks of Volcano Island and offshore of the eastern flank of Volcano Island, are solutions from time periods of transition between inflation and deflation when there is little cumulative deformation and therefore no signal to model. In general, deflationary sources cluster just east and southeast of the Main Crater, and inflationary sources cluster just northeast of the Main Crater. Deflationary sources cluster around 4 km depth, with a slight apparent deepening throughout the period (Figure 11). Inflationary sources cluster around 5–6 km depth, consistent with the depths of local seismic events during this time period located by PHIVOLCS (Figure 11). Sources appear to shallow in transitional periods. Such deviations in source depth from the 4–6 km range may represent true migration of the source, but more likely reflect weaknesses in the model resulting from modeling of periods of marginally significant velocities. Most of the time-variable sources fall within the 95% confidence bounds of the average of the 1999 deflationary and 2000 inflationary sources, indicating that the sources responsible for deformation during this time period are indistinguishable within our confidence estimates. The time variability of the deformation behavior described here likely results from changes within a single,

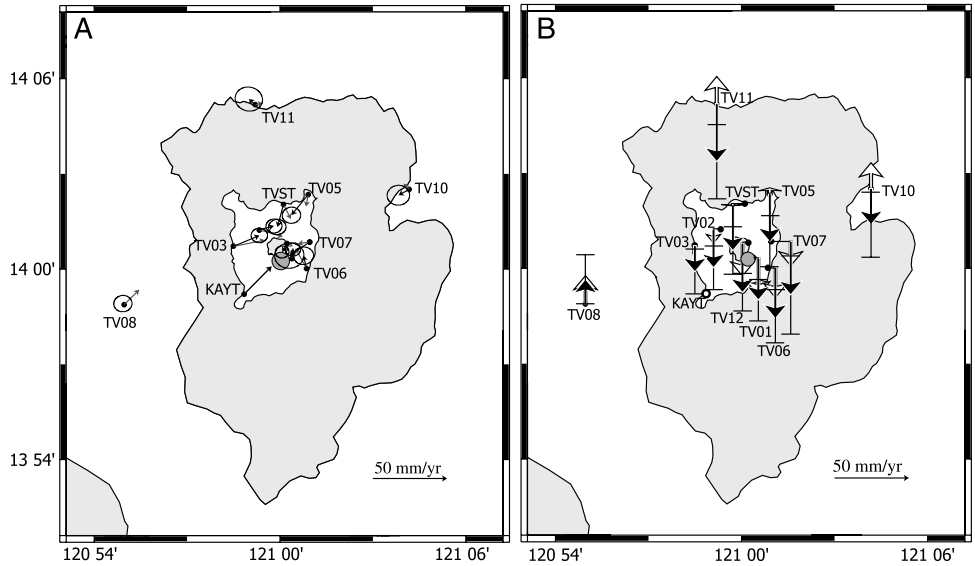

Figure 7. Velocities and model results, deflationary trend, 13 June to 30 December 1999. Gray circle represents source location. (a) Horizontal velocities. Observed velocities and 95% confidence estimates are shown in black; model velocities are shown in gray. An average network velocity has been calculated and removed from each site relative to KAYT. This average velocity is represented in opposite polarity as the velocity of KAYT. (b) Vertical velocities. Observed velocities and 95% confidence estimates are shown in black; model velocities are shown in white. The time period modeled is shown in Figure 6.

stationary source, as opposed to multiple sources or source migration.

8. Discussion

[22] Surface deformation can be ascribed to a wide variety of tectonic, magmatic, hydrothermal, and surficial processes. Several key observations lead us to the conclusion that the crustal motions recorded at Taal are largely related to magmatic processes: (1) deformation is time-variable but persists on timescales of days to months; (2) deformation is volcano-wide and roughly radial to the volcano's center; (3) the deformation patterns are well modeled by a Mogi point source at ~4–6 km depth; (4) deformation changes polarity from inflation to deflation, without seasonal cyclicity or correlation with rainfall or other environmental factors; and (5) both episodes of inflation begin and end abruptly, with transition times of <1 week. These deformation patterns could result from pressure changes within a hydrothermal and/or a magmatic

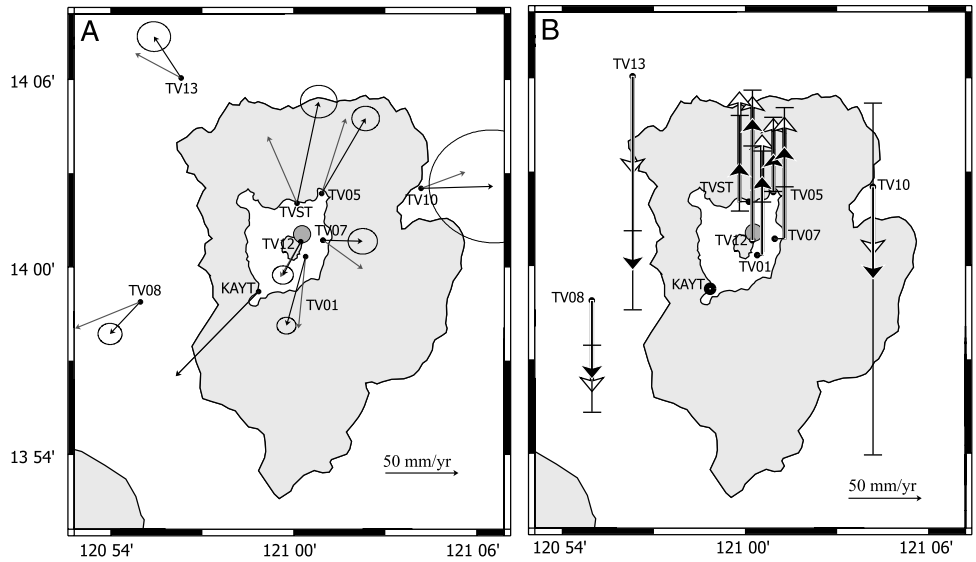

Figure 8. Velocities and model results, inflationary trend, 2 March to 8 October 2000. (a) Horizontal velocities. (b) Vertical velocities. Symbols as described in Figure 7.

Table 1. Station Velocities Relative to KAYT [a]

Stn.	Longitude	Latitude	Ve	Vn	Vu	σe	σn	Corr.[b]	σu
Deflationary Trend (*13 June to 30 Dec. 1999*) *Observed Velocities*									
PINT	121.0159	14.0142	−32	−28	−36	4	3	0.026	11
TV01	121.0064	14.0055	−18	−12	−28	2	2	0.033	6
TV02	120.9889	14.0206	−9	−16	−26	2	2	0.027	6
TV03	120.9729	14.0120	−1	−11	−18	2	2	0.013	6
TV05	121.0152	14.0391	−30	−32	−32	3	2	0.019	7
TV06	121.0143	14.0004	−20	−10	−34	3	2	0.025	7
TV08	120.9161	13.9814	−19	−18	17	3	2	0.020	7
TV10	121.0695	14.0419	−26	−23	−24	3	3	0.017	8
TV11	120.9867	14.0844	−23	−15	−39	4	3	−0.063	10
TV12	121.0037	14.0134	−22	−24	−33	2	2	0.033	5
TVST	121.0018	14.0340	−22	−34	−32	2	2	0.027	7
Deflationary Trend (*13 June to 30 Dec. 1999*) Model Velocities									
PINT			−26	−20	−16				
TV01			−18	−11	−26				
TV02			−3	−23	−9				
TV03			3	−14	0				
TV05			−20	−27	4				
TV06			−26	−5	−20				
TV08			−8	−9	19				
TV10			−22	−15	17				
TV11			−13	−18	18				
TV12			−14	−20	−22				
TVST			−13	−28	−2				
Inflationary Trend (*2 March to 8 October 2000*) Observed Velocities									
TV01	121.0064	14.0055	44	11	54	3	2	−0.003	7
TV05	121.0152	14.0391	87	109	26	4	3	−0.004	10
TV07	121.0160	14.0142	84	57	63	4	4	0.006	11
TV08	120.9161	13.9814	36	36	−54	3	3	−0.007	9
TV10	121.0695	14.0419	106	59	−63	18	16	−0.022	49
TV12	121.0037	14.0134	45	35	83	3	3	0.001	8
TV13	120.9384	14.1008	38	86	−132	5	4	−0.016	11
TVST	121.0018	14.0340	71	127	26	5	5	0.000	14
Inflationary Trend (*2 March to 8 October 2000*) Model Velocities									
TV01			52	9	82				
TV05			73	109	50				
TV07			84	38	83				
TV08			12	40	−62				
TV10			87	69	−46				
TV12			43	34	98				
TV13			25	75	−66				
TVST			37	104	75				

[a]Velocities in mm/yr.
[b]Correlation coefficient.

system, but the predominant inflationary behavior of the system suggests that magmatic recharge plays a significant role.

[23] The deformation pattern observed over the last 3.5 years at Taal is remarkably similar to that observed over the last three decades at Campi Flegrei caldera. Both volcanoes are characterized by rapid uplift followed by more gradual subsidence, although episodes of inflation at Campi Flegrei have persisted over timescales up to three times the inflationary periods at Taal and rates of maximum uplift are more than 3 times those at Taal. *Gaeta et al.* [1998] demonstrated that a hydrothermal system contributes significantly to volcano deformation at Campi Flegrei and at other large calderas. They point out, however, that changes within the hydrothermal system accounting for deformation at Campi Flegrei most probably are a direct response to changes within the magmatic system. *Dvorak and Dzurisin* [1997] attribute uplift epi-

Table 2. Mogi Source Model Parameters for Major Deflationary and Inflationary Trends

Model	Latitude, °N	Range, °N	Longitude, °E	Range, °E	Depth, km	Depth Range, km	Volume,[a] km^3/yr	Volume Range, km^3/yr	MSE
Starting model	14.020		121.000		20.0		−0.020		
Deflation	14.005	13.988–14.020	121.004	120.988–121.020	4.2	2.2–7.8	−0.004	−0.015 to −0.001	9.8554
Inflation	14.018	14.008–14.027	121.005	120.993–121.024	5.2	3.2–9.1	0.020	0.006–0.090	15.4785

[a]Volume represents rate of volume flux, taken as two thirds of the volume of surface displacement.

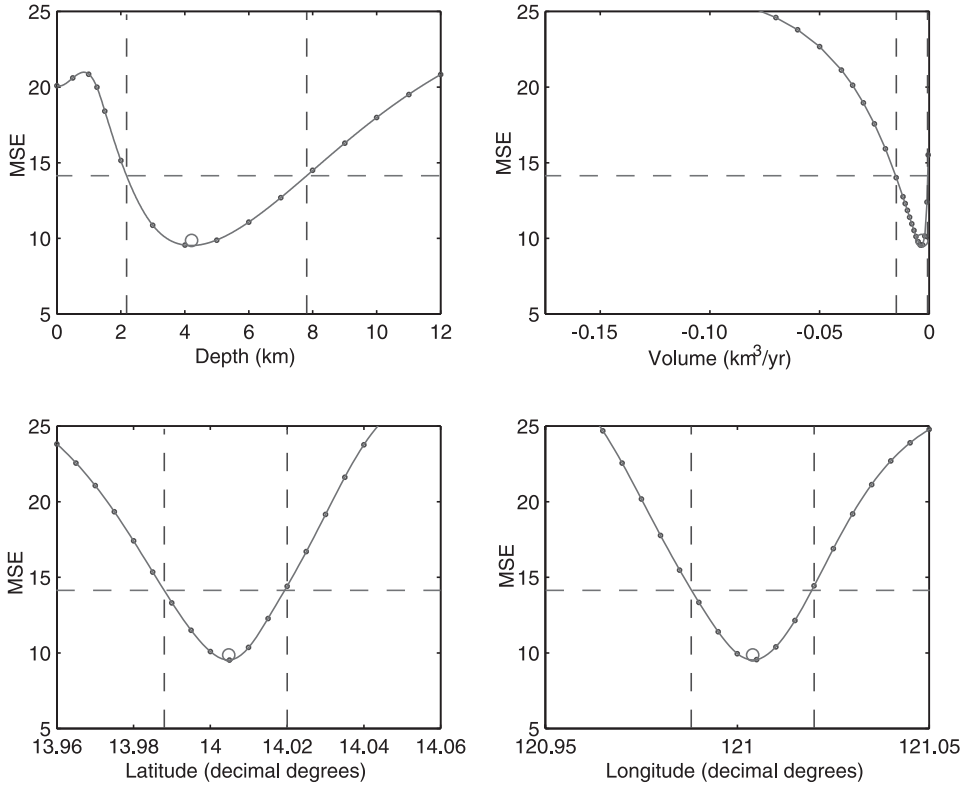

Figure 9. Mean square error (MSE) versus model parameters, deflationary trend. Curves were obtained by holding the parameter in question fixed while solving for the other three (values represented by small circles). Large circles represent the model solution as shown in Figure 7, obtained by solving for all for parameters simultaneously. Horizontal dashed lines represent the 95% confidence range of MSE values as determined based on a χ^2 distribution. Vertical dashed lines represent the resulting 95% confidence range of each model parameter.

sodes at Long Valley, Campi Flegrei, and Rabaul calderas to magmatic intrusions, based on the abrupt initiation of uplift. Gravity gradients associated with uplift episodes at these volcanoes are consistent with the migrating fluid having a density equivalent to basaltic magma [*Battaglia et al.*, 1999; *Berrino*, 1994; *McKee et al.*, 1989]. Gravity has not been measured at Taal to independently confirm magmatic intrusion. However, the similarity of inflationary episodes at Taal Volcano to those observed at other major calderas, coupled with the timing relationship of changes in the deformation behavior to changes in surface hydrothermal behavior, suggests that inflation episodes at Taal initiate as magmatic intrusions, which are then followed by changes in hydrothermal circulation. *Dvorak and Dzurisin* [1997] argue that because both the addition of fluids and the transfer of heat into a confined aquifer are diffusive processes, the resulting pressure change within the hydrothermal system should be gradual, with the transition times in deformation patterns limited by the ability of fluids to change circulation patterns within the crust. Transitions may occur over timescales of months to years. The initiation of magma movement, on the other hand, is known to occur quite rapidly. Magmatic intrusion is also the most plausible explanation for the lack of deflationary recovery following the February–November 2000 inflation event at Taal (the postinflationary level has been sustained for nearly 2 years at the time of this writing).

[24] If inflation initiates as magmatic intrusion into a shallow reservoir, we can infer characteristics of both the geometry and the recharge behavior of Taal's shallow magmatic system. Modeling suggests the source of recent deformation is centered beneath Volcano Island at ~5 km depth. This depth is consistent with the geodetically inferred depths of magma bodies at other basaltic volcanoes including Cerro Azul, Galapagos (5 km [*Amelung et al.*, 2000]), at intermediate composition volcanoes such as Hekla, Iceland (5–6 km [*Tryggvason*, 1994]), and also at several large silicic calderas, including Yellowstone (3–6 km [*Vasco et al.*, 1990]) and Long Valley (5–7 km [*Langbein et al.*, 1995]). A volume increase rate of ~0.020 km^3/yr was estimated for the 2000 uplift (2 March to 8 October 2000) at Taal (Table 2). This presumably reflects magma flux rate, although the true rate may be larger if inelastic effects are important, or smaller if the hydrothermal system contributes to inflation. We can infer a total volume change during the 2000 inflation event of ~0.015 km^3, halfway between estimated eruptive volumes during the phreatomagmatic eruptions of Taal in 1965 (0.022 km^3) and 1966 (0.010 km^3) [*Philippine Institute of Volcanology and Seismology*, 1995]. If recent behavior is indicative of long-term behavior at Taal, recharge into a shallow crustal reservoir occurs episodically and irregularly, with the duration and volume of intrusion varying from one recharge episode to the next.

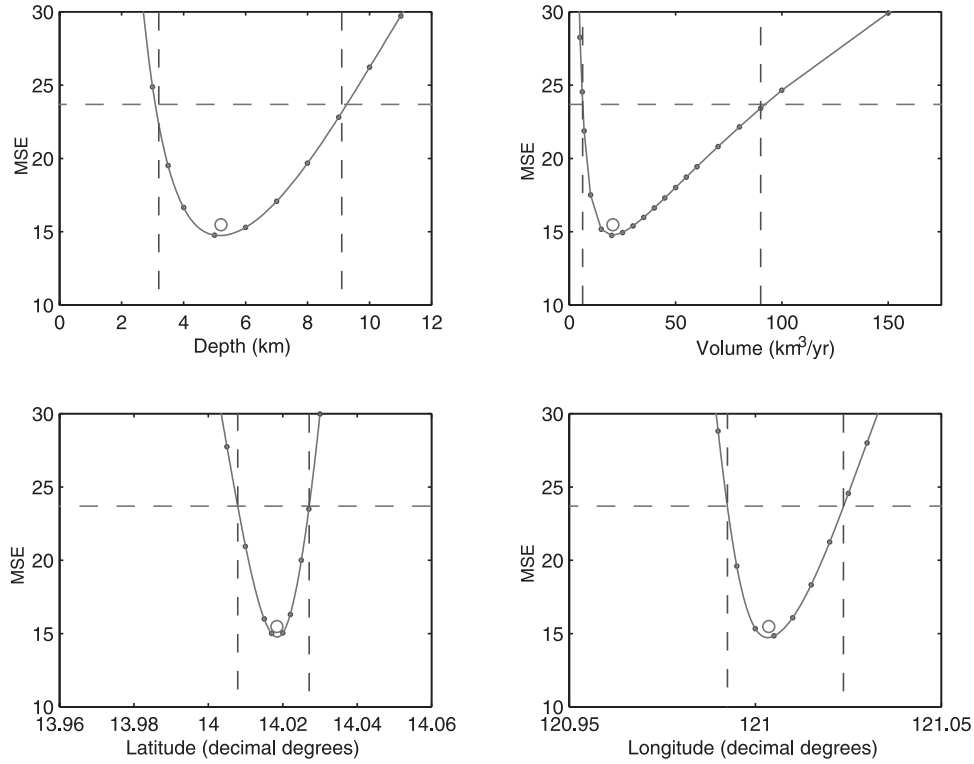

Figure 10. Mean square error (MSE) versus model parameters, inflationary trend. Symbols as described in Figure 9.

[25] Deflationary trends at Taal have been irregular, characterized by varying rates and an inconsistent relationship to prior inflation. The volume of the 1999 deflation appears to roughly equal that of the preceding inflation, but deflation following the 2000 inflation event was brief and accounts for less than 30% of the preceding inflation (Figure 4). *Dvorak and Dzurisin* [1997] suggested that, although local contraction by cooling and regional exten-

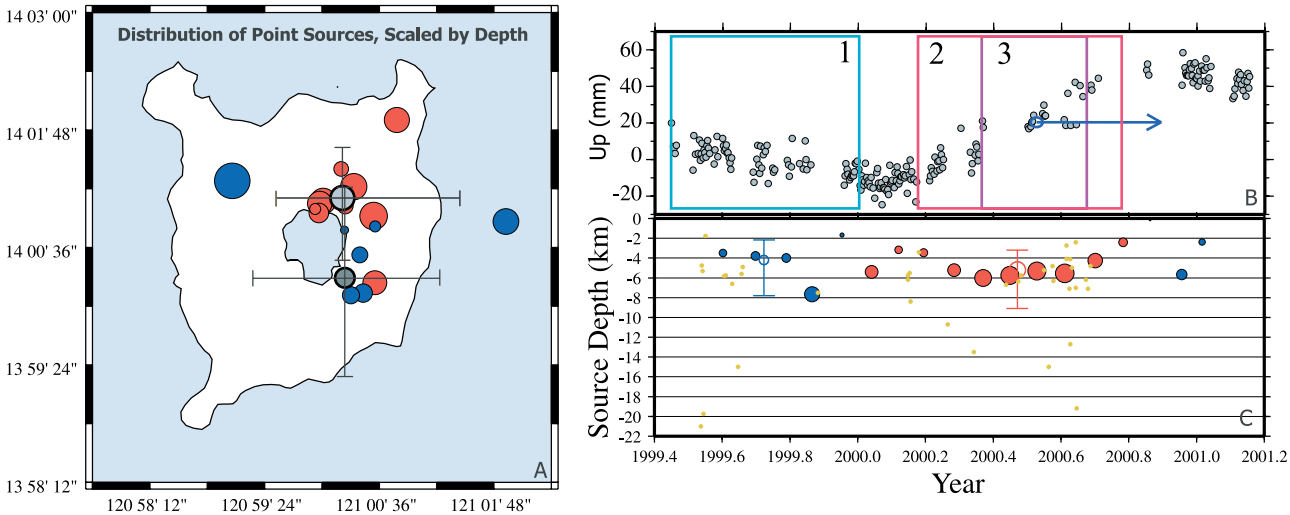

Figure 11. Inversion results for a running, 4-month time window, June 1999 to February 2001. (a) Map view of source locations, scaled by depth. Deflationary sources are shown in blue; inflationary sources are shown in red. The sources determined for the entire deflationary and inflationary periods shown in Figures 7 and 9 are shown as light blue and open circles, respectively, with 95% confidence estimates. (b) Vertical coordinate component of TV12 relative to KAYT shown for reference, along with the time windows used to model the deflationary (1) and inflationary (2) trends and the width of the running 4-month time window (3). (c) Source depths versus time, scaled by volume. Sources as in Figure 11a. Each source is centered at the mean value of the time period modeled. Small yellow circles represent seismic events located by PHIVOLCS.

Table 3. Mogi Source Model Parameters for the Period June 1999 to March 2001

Time Period							
Start Date	End Date	Median Day	Latitude, °N	Longitude, °E	Depth, km	Volume,[a] km^3/yr	MSE
13 June 1999	4 Oct. 1999	1999.603	14.009	121.007	3.5	−0.002	8.3
13 July 1999	12 Nov. 1999	1999.699	14.002	121.005	3.8	−0.003	10.5
13 Aug. 1999	14 Nov. 1999	1999.789	14.002	121.007	4.0	−0.003	4.2
13 Sept. 1999	12 Jan. 2000	1999.866	14.021	120.984	7.7	−0.016	5.0
16 Oct. 1999	12 Feb. 2000	1999.953	14.013	121.004	1.7	−0.000	2.9
13 Nov. 1999	18 March 2000	2000.041	14.032	121.013	5.4	0.010	3.3
16 Dec. 1999	12 April 2000	2000.121	14.023	121.003	3.2	0.002	2.2
13 Jan. 2000	9 May 2000	2000.196	14.017	121.004	3.5	0.003	6.7
13 Feb. 2000	12 June 2000	2000.285	14.004	121.009	5.2	0.009	7.7
17 March 2000	12 July 2000	2000.370	14.015	121.009	6.0	0.024	7.2
13 April 2000	11 Aug. 2000	2000.449	14.020	121.006	5.7	0.027	4.2
13 May 2000	8 Sept. 2000	2000.529	14.017	121.000	5.3	0.028	3.4
13 June 2000	8 Oct. 2000	2000.611	14.018	121.000	5.6	0.032	2.9
13 July 2000	12 Nov. 2000	2000.701	14.016	120.999	4.3	0.014	2.3
13 Aug. 2000	12 Dec. 2000	2000.784	14.017	120.999	2.4	0.003	2.2
08 Sept. 2000	12 Jan. 2001	2000.863	14.037	121.003	0.1	−0.000	1.4
16 Oct. 2000	12 Feb. 2001	2000.956	14.014	121.032	5.6	−0.005	1.5
13 Nov. 2000	1 March 2001	2001.016	14.014	121.009	2.4	−0.001	1.0

[a]Volume represents rate of volume flux, taken as two thirds of the volume of surface displacement.

sion may contribute to subsidence observed at major calderas such as Campi Flegrei, the dominant mechanism of subsidence is probably exsolution of magmatic fluids from the magma body into the overlying hydrothermal system. *Gaeta et al.* [1998] observed that deflation at Campi Flegrei is rapid immediately following inflation, and continues at a decreasing rate until reaching a long-term deflation rate that is characteristic for the caldera. The decrease in rate supports the hypothesis that initial deflation occurs in response to the process responsible for inflation. Unlike at Campi Flegrei, deflation at Taal does not decay but begins slowly and continues at an irregular rate. Still, exsolution of fluids or gases from a magma chamber can explain similarity of the locations of deflationary and inflationary sources during the 1994 crisis [*Thibault*, 1999] and the deformation events analyzed here. A careful analysis combining lake chemistry data and deformation data may help to clarify the mechanism for deflation.

8.1. Implications for Monitoring and Eruption Forecasting

[26] Recent deformation measurements at Taal indicate that sustained inflation on timescales of weeks to months does not necessarily lead directly to eruption. We infer that the inflationary behavior observed represents routine recharge of a shallow magma body. Understanding whether behavior leading to eruptions differs from that during these routine recharge events is critical in forecasting eruptions. Historically, eruptions at Taal have been preceded by weeks to months of increased seismicity, rapid deformation, increased temperature of lake or hydrothermal waters, increased hydrothermal activity, and changes in lake chemistry and/or color. Changes in these parameters during the time period studied (1999–2001) were short-lived and uncorrelated with deformation. We thus expect that changes within the magmatic system that are precursors to eruption are likely to differ from the processes observed during the period of study. Changes in deformation behavior signaling an imminent eruption might include an increase in uplift rate and localization of the deformation pattern as magma moves to shallower levels. The spatial and temporal density of GPS networks at Taal should readily resolve these types of precursors.

9. Conclusions

[27] The current Taal GPS networks provide nearly unprecedented spatial and temporal density of deformation measurements, revealing highly time-variable deformation behavior that is similar to that observed at other large calderas. The Taal network represents one of the first deployments of single-frequency GPS receivers as a volcano-monitoring tool. Results presented here indicate that east and vertical coordinate scatter is only slightly lower in the dual-frequency data than in the single-frequency data. The relatively high coordinate scatter in the north component of single-frequency solutions is a direct function of distance north from the base station, reflecting the high north-south ionospheric gradient expected at low latitudes. Despite the scatter, deformation is clearly resolved in all three components of measurement. This study indicates that both dual- and single-frequency GPS systems are capable of resolving vertical motions, and that single-frequency GPS systems are viable high-precision, low-cost volcano-monitoring geodetic networks.

[28] Deformation during the time period studied includes deflation punctuated by two periods of inflation, from approximately January to March 1999 and February to November 2000. The second period of inflation was characterized by approximately 120 mm of uplift of the center of Volcano Island relative to the northern caldera rim, at rates up to 216 mm/yr. The duration of deformation trends ranges from 1 to 9 months. These timescales are significantly shorter than previous episodic measurement intervals at Taal including campaign GPS measurements, leveling, and EDM, highlighting the importance of continuous measurement.

[29] We interpret the inflationary episodes as initiating by intrusion of magma into a shallow reservoir. Deflation probably results from exsolution of magmatic fluids and/or gases from the cooling intrusion. Simple point source modeling of the second inflationary period (2 March to

8 October 2000) yields a source depth of 5.2 km, with a 95% confidence range of 3.2–9.1 km, suggesting a magma reservoir within this depth range. Similar modeling of the preceding deflationary trend (13 June to 30 December 1999) yields a source depth of 4.2 km, with a 95% confidence range of 2.2 to 7.8 km, indicating the deflationary source is very near, or the same as, the source of inflation. Modeling of these same time periods using a running, 4-month time window reveals no conclusive evidence for migration of the source during either trend, indicating that changes in the deformation pattern result from changes within a single source as opposed to source migration. Preliminary modeling of more complicated sources suggests that the inflationary reservoir or system of reservoirs is elongate in a northwest-southeast direction. The relationship between seismicity and deformation suggests changes within the magmatic system may be evident in the deformation data long before they are expressed in the seismic data. We expect that changes within the magmatic system leading to eruption will result in precursory deformation measurable by the current Taal GPS network.

[30] **Acknowledgments.** We are deeply indebted to the field crew of the PHIVOLCS Volcano Monitoring and Eruption Prediction Division, without whose efforts this experiment could never have succeeded. We acknowledge in particular the work of Agnes Aguilar, Elmer Gabinete, Emmanuel Sexon, Ricardo Saeta, and Manuel Isada. We are grateful to PHIVOLCS' director, Raymundo Punongbayan, for his continued support for the project, and to Emmanuel Ramos for his efforts in organizing the initial GPS work at Taal. We also acknowledge the support of the UNAVCO facility throughout this project, including the superb engineering efforts of Oivind Ruud, Spencer Reeder, Chuck Kurnik, Jay Sklar, and Karl Feaux, and archiving support from Dave Maggert and Fran Boler. John Braun and Teresa Van Hove provided valuable data processing expertise. We thank referees Chris Newhall and Tim Dixon, along with Associate Editor Freysteinn Sigmundsson, for their insightful reviews, and Gary Pavlis for comments on an earlier version of this manuscript. This work was supported by National Science Foundation grants EAR-0073992 and EAR-9727300, and NASA grant NAG5-8582 to M. Hamburger and NASA grant NRA-96-MTPE-05 to C. Meertens.

References

Alcaraz, A., Surveillance of Taal Volcano, *Philipp. Geol.*, *20*, 1–13, 1966.

Alcaraz, A., and R. Datuin, Geothermal phenomena of the 1965 phreatomagmatic eruption of Taal Volcano, *J. Geol. Soc. Philipp.*, *28*, 31–40, 1974.

Amelung, F., S. Jónsson, H. Zebker, and P. Segall, Widespread uplift and 'trapdoor' faulting on Galápagos volcanoes observed with radar interferometry, *Nature*, *407*, 993–996, 2000.

Barberi, F., G. Corrado, F. Innocenti, and G. Luongo, Phlegraean Fields 1982–1984: Brief chronicle of a volcano emergency in a densly populated area, *Bull. Volcanol.*, *47*, 175–185, 1984.

Bartel, B. A., Magma dynamics at Taal Volcano, Philippines from continuous GPS measurements, M.S. thesis, 168 pp., Dep. of Geol. Sci., Indiana Univ., Bloomington, 2002.

Bartel, B., M. Hamburger, A. Lowry, C. Meertens, S. Reeder, C. Thibault, E. Ramos, E. Corpuz, E. Gabinete, M. Sexon, and A. Aguilar, GPS measurement of volcanic deformation at Taal Volcano, Philippines (abstract), *Eos Trans. AGU*, *80*(46), Fall Meet. Supp., F272, 1999.

Battaglia, M., C. Roberts, and P. Segall, Magma intrusion beneath Long Valley caldera confirmed by temporal changes in gravity, *Science*, *285*, 2119–2122, 1999.

Beck, J. V., and K. J. Arnold, *Parameter Estimation in Engineering and Science*, John Wiley, Hoboken, N. J., 1977.

Berrino, G., Gravity changes induced by height-mass variations at the Campi Flegrei caldera, *J. Volcanol. Geotherm. Res.*, *61*, 293–309, 1994.

Besana, G. M., T. Shibutani, N. Hirano, M. Ando, B. Bautista, I. Narag, and R. S. Punongbayan, The shear wave velocity structure of the crust and uppermost mantle beneath Tagaytay, Philippines inferred from receiver function analysis, *Geophys. Res. Lett.*, *22*, 3143–3146, 1995.

Beutler, G., J. Kouba, and T. Springer, Combining the orbits of the IGS Analysis Centers, *Bull. Geod.*, *69*, 200–222, 1995.

Cabral-Cano, E., T. Dixon, C. Meertens, and F. Correa-Mora, Surface deformation on active volcanoes in Central Mexico, paper presented at 1999 UNAVCO Volcano Geodesy Workshop, Jackson, Wyo., 1999.

Castle, R. O., J. E. Estrem, and J. C. Savage, Uplift across Long Valley caldera, California, *J. Geophys. Res.*, *89*, 11,507–11,516, 1984.

Cervelli, P., P. Segall, F. Amelung, H. Garbeil, C. Meertens, S. Owen, A. Miklius, and M. Lisowski, The 12 September 1999 Upper East Rift Zone dike intrusion at Kilauea Volcano, Hawaii, *J. Geophys. Res.*, *107*(B7), 2150, doi:10.1029/2001JB000602, 2002.

Defant, M. J., J. Z. de Boer, and D. Oles, The Western Central Luzon volcanic arc, the Philippines: Two arcs divided by rifting?, *Tectonophysics*, *145*, 305–317, 1988.

Dvorak, J. J., and D. Dzurisin, Volcano geodesy: The search for magma reservoirs and the formation of eruptive vents, *Rev. Geophys.*, *35*, 343–384, 1997.

Gabinete, E., Interpretation of the 1992 and 1994 ground deformation data at Taal Volcano, Batangas, paper presented at in-house workshop, Philipp. Inst. of Volcanol. and Seismol., Quezon City, 1999.

Gaeta, F. S., G. De Natale, F. Peluso, G. Mastrolorenzo, D. Castagnolo, C. Troise, F. Pingue, D. G. Mita, and S. Rossano, Genesis and evolution of unrest episodes at Campi Flegrei caldera: The role of thermal fluid-dynamical processes in the geothermal system, *J. Geophys. Res.*, *103*, 20,921–20,933, 1998.

Hugentobler, U., S. Schaer, and P. Fridez (Eds.), *Bernese GPS Software Version 4.2*, 515 pp., Astron. Inst., Univ. of Berne, Berne, Switzerland, 2001.

Kelley, M. C., *The Earth's Ionosphere: Plasma Physics and Electrodynamics*, 487 pp., Academic, San Diego, Calif., 1989.

Langbein, J., D. P. Hill, T. N. Parker, and S. K. Wilkinson, An episode of reinflation of the Long Valley caldera, eastern California: 1989–1991, *J. Geophys. Res.*, *98*, 15,851–15,870, 1993.

Langbein, J. O., D. Dzurisin, G. Marshall, R. Stein, and J. Rundle, Shallow and peripheral volcanic sources of inflation revealed by modeling two-color geodimeter and leveling data from Long Valley caldera, California, 1988–1992, *J. Geophys. Res.*, *100*, 12,487–12,495, 1995.

Listanco, E., Space-time patterns in the geologic and magmatic evolution of calderas: A case study at Taal Volcano, Philippines, Ph.D. thesis, Tokyo Univ., Tokyo, 1994.

Lowry, A. R., M. W. Hamburger, C. M. Meertens, and E. G. Ramos, GPS monitoring of crustal deformation at Taal Volcano, Philippines, *J. Volcanol. Geotherm. Res.*, *105*, 35–47, 2001.

McKee, C., J. Mori, and B. Talai, Microgravity changes and ground deformation at Rabaul Caldera, 1973–1985, in *Volcanic Hazards: Assessment and Monitoring*, edited by J. H. Latter, pp. 399–428, Springer-Verlag, New York, 1989.

Meertens, C. M., C. Rocken, J. Braun, W. Shiver, R. Ware, T. VanHove, D. Mencin, and L. Estey, Development of dense low cost GPS networks for crustal deformation monitoring and water vapor tomography (abstract), *Eos Trans. AGU*, *79*(24), West. Pac. Geophys. Meet. Suppl., W11, 1998.

Meertens, C. M., J. Braun, D. Mencin, C. Conquest, and L. Estey, Development of a low cost single-frequency GPS system for volcano deformation monitoring, paper presented at 1999 UNAVCO Volcano Geodesy Workshop, Jackson, Wyo., 1999.

Miklius, A., M. F. J. Flower, J. P. P. Huijsmans, S. B. Mukasa, and P. Castillo, Geochemistry of lavas from Taal Volcano, southwestern Luzon, Philippines: Evidence for multiple magma supply systems and mantle source heterogeneity, *J. Petrol.*, *32*, 593–627, 1991.

Mogi, K., Relations between the eruptions of various volcanoes and the deformation of the ground surface around them, *Bull. Earthquake Res. Inst. Univ. Tokyo*, *36*, 99–134, 1958.

Moore, J. G., K. Nakamura, and A. Alcaraz, The 1965 eruption of Taal Volcano, *Science*, *151*, 955–960, 1966.

Newman, A. V., T. H. Dixon, G. I. Ofoegbu, and J. E. Dixon, Geodetic and seismic constraints on recent activity at Long Valley Caldera, California: Evidence for viscoelastic rheology, *J. Volcanol. Geotherm. Res.*, *105*, 183–206, 2001.

Nishigami, K., et al., Shallow crustal structure beneath Taal volcano, Philippines, revealed by the Seismic Explosion Survey, *Bull. Disaster Prev. Res. Inst. Kyoto Univ.*, *44*, 123–138, 1994.

Philippine Institute of Volcanology and Seismology, Taal Volcano profile, report, 41 pp., Quezon City, 1995.

Punongbayan, R. S., and R. I. Tilling, Recent case histories, in *Volcanic Hazards*, *Short Course Geol.*, vol. 1, edited by R. I. Tilling, pp. 81–101, AGU, Washington, D. C., 1989.

Rabaul Volcano Observatory, *Bulletin of the Global Volcanism Network*, *19*(1), 1994. (Available at http://www.volcano.si.edu/gvp/world/region05/new_brit/rabaul/bgvn_1901)

Schaer, S., G. Beutler, M. Rothacher, and T. A. Springer, Daily global ionosphere maps based on GPS carrier phase data routinely produced

by the code analysis center, paper presented at the IGS AC Workshop, Inst. of Geol. Sci., Silver Spring, Md., 19–21 March 1996.

Thibault, C. A., GPS measurements of crustal deformation in the northern Philippine Island Arc, M.S. thesis, 126 pp., Dep. of Geol. Sci., Indiana Univ., Bloomington, 1999.

Tieman, A. K., The 1994 seismic swarm at Taal Volcano, Philippines, undergraduate research thesis, 47 pp., Dep. of Geol. Sci., Indiana Univ., Bloomington, 1999.

Torres, R. C., S. Self, and R. S. Punongbayan, Attention focuses on Taal: Decade volcano of the Philippines, *Eos Trans. AGU*, *76*, 241, 246–247, 1995.

Tryggvason, E., Observed ground deformation at Hekla, Iceland prior to and during the eruptions of 1970, 1980–1981 and 1991, *J. Volcanol. Geotherm. Res.*, *61*, 281–291, 1994.

Vasco, D. W., R. B. Smith, and C. L. Taylor, Inversion of sources of crustal deformation and gravity change at the Yellowstone caldera, *J. Geophys. Res.*, *95*, 19,839–19,856, 1990.

Wolfe, J. A., and S. Self, Structural lineaments and Neogene volcanism in southwestern Luzon, in *The Tectonic and Geologic Evolution of Southeast Asian Seas and Islands: Part 2*, *Geophys. Monogr. Ser.*, vol. 27, edited by D. Hayes, pp. 157–172, AGU, Washington, D. C., 1983.

B. A. Bartel and C. M. Meertens, UNAVCO, Inc., P.O. 6350 Nautilus Drive, Boulder, CO 80307, USA. (bartel@unavco.org)

E. Corpuz, Philippine Institute of Volcanology and Seismology, Department of Science and Technology, C.P. Garcia Ave., U.P. Diliman, Quezon City, Philippines. (ecorpuz@phivolcs.dost.gov.ph)

M. W. Hamburger, Department of Geological Sciences, Indiana University, 1001 East Tenth St., Bloomington, IN 47405, USA. (hamburg@indiana.edu)

A. R. Lowry, Department of Physics, University of Colorado, Campus Box 390, Boulder, CO 80309, USA. (arlowry@himalaya.colorado.edu)